

MOTION PLANNING AND FEEDBACK CONTROL FOR A UNICYCLE IN A WAY POINT FOLLOWING TASK: THE VFO APPROACH

MACIEJ MICHAŁEK, KRZYSZTOF KOZŁOWSKI

Chair of Control and Systems Engineering
Poznań University of Technology, Piotrowo 3A, 60–965 Poznań, Poland
e-mail: {maciej.michalek, krzysztof.kozlowski}@put.poznan.pl

This paper is devoted to the *way point following* motion task of a unicycle where the motion planning and the closed-loop motion realization stage are considered. The *way point following* task is determined by the user-defined sequence of way-points which have to be passed by the unicycle with the assumed finite precision. This sequence will take the vehicle from the initial state to the target state in finite time. The motion planning strategy proposed in the paper does not involve any interpolation of way-points leading to simplified task description and its subsequent realization. The motion planning as well as the motion realization stage are based on the Vector-Field-Orientation (VFO) approach applied here to a new task. The unique features of the resultant VFO control system, namely, predictable vehicle transients, fast error convergence, vehicle *directing effect* together with very simple controller parametric synthesis, may prove to be useful in practically motivated motion tasks.

Keywords: unicycle, way point following, motion planning, feedback control, vector fields.

1. Introduction

In the robotics literature, one usually distinguishes three basic and uniquely defined control tasks (de Luca *et al.*, 1998): trajectory tracking, path following, and posture stabilization (set-point regulation). However, in practice, mobile robot control tasks cannot be easily and definitely classified into one of these types (Lawrence *et al.*, 2008). For instance, one can find practical motion problems like tracking a leading vehicle where its instantaneous motion cannot be anticipated, or the task of motion with the target not defined in advance but determined by defining the desired azimuthal direction and longitudinal robot velocity, or finally the task of motion along the geometrical contour not known in advance, like the *wall-following* problem (Siegwart and Nourbakhsh, 2004). Moreover, sometimes even if a particular task belongs to one of the first two types mentioned above, its full description in terms of the reference full-state trajectory or geometrical path can be a nontrivial algorithmic problem, especially in the case of motion planning in a cluttered environment (Madi, 2004). Thus it seems to be desirable to propose an alternative method of motion task determination, which would combine two useful features, namely, the simplicity of task description characteristic for the set-point regulation prob-

lem together with the ability of shaping the robot's path which is intrinsic to the path following motion problem. One of the simplest methods consists in the determination of the set \mathcal{S}_t , which is made of the way-point sequence along with the initial (starting) state and the target (final) state. The set \mathcal{S}_t can be treated as a simplified definition of the desired path assuming that the way-points are chosen sufficiently close to each other and the vehicle motion between them is predictable and sufficiently smooth. Simplified task determination might turn out to be computationally efficient and useful for simple motion re-planning by adding way-points to the set \mathcal{S}_t even already during task realization.

The planning problem for motion described by the set of way-points can be solved in many ways. The shortest path with finite curvature connecting the way-points is made of the sequence of arcs and rectilinear segments (Reeds and Shepp, 1990). Planning the motion involves finding and combining the finite sequence of the mentioned primitives leading to the resultant curve with a discontinuous curvature. The smoothing procedure proposed in (Scheuer and Fraichard, 1997) and (Fleury *et al.*, 1995), where clothoid segments were used in the neighborhoods of discontinuity points, can improve the quality of planned motion. However, the above approaches finally lead to

geometrical paths determined using an interpolation procedure between the way-points. As a consequence, the control task becomes the path following problem and the feature of simplified task definition may be lost. Moreover, as mentioned in (Samson, 1992), path following task realization usually involves the determination of the instantaneous *perpendicular distance* to the path, which is generally a non-trivial or even a non-unique mathematical problem. Thus, the issue of simplified task determination, which does not involve extending it to the full path, together with simplified motion realization seems to be an open research problem.

This paper proposes an alternative algorithm of motion planning in a free space using only the sequence of defined and recomputed way-points. The method does not involve an extension to any geometrical path preserving the simplicity of the task in a sense of its description as well as realization. The finite-time motion control problem (with the motion time-horizon being a function of controller parameters) is solved by a modified version of the original Vector-Field-Orientation (VFO) feedback controller presented by the authors in (Michałek and Kozłowski, 2009), but designed here with a strict connection to the newly proposed planning method. The motion task proposed and subsequently accomplished by the strategy introduced in this paper will be called *way point following*¹. The name emphasizes the combination of features characteristic for set-point regulation and partially for the path following problem, leading, however, to simplified version of the latter.

The paper is an extension of the preliminary work (Michałek and Kozłowski, 2008) and is organized as follows: Section 2 introduces basic assumptions, includes the system model and the task definition considered. A brief explanation of the original VFO control approach for posture stabilization is presented in Section 3. The motion planning algorithm and the VFO motion control strategy are the main topic of Sections 4 and 5, respectively. Section 6 illustrates simulation results. Conclusions are given in Section 7.

2. Problem formulation

2.1. Unicycle model. The vehicle model taken into account in the paper is a unicycle with the following kinematics:

$$\dot{\mathbf{q}}(\tau) = \begin{bmatrix} 1 \\ 0 \\ 0 \end{bmatrix} u_1(\tau) + \begin{bmatrix} 0 \\ \cos \theta(\tau) \\ \sin \theta(\tau) \end{bmatrix} u_2(\tau), \quad (1)$$

where $\mathbf{q} \triangleq [\theta \ x \ y]^T = [\theta \ \mathbf{q}^{*T}]^T \in \mathbb{R}^3$ is a state vector describing the orientation angle and the position vector of a local frame attached to the unicycle (see Fig. 1). The

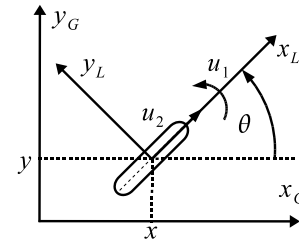


Fig. 1. Unicycle in the global frame $\{G\}$.

control inputs $u_1, u_2 \in \mathbb{R}$ can be interpreted as angular and longitudinal velocity, respectively.

2.2. Way point following motion task. Here we provide the mathematical background for the *way point following* motion task. Let us introduce the following set of finite number of way-points:

$$\mathcal{S}_t \triangleq \{\mathbf{q}_{t0}, \mathbf{q}_{t1}, \mathbf{q}_{t2}, \dots, \mathbf{q}_{tN}\}, \quad (2)$$

which have to be passed by the unicycle (with assumed precision) during the motion task considered, with \mathbf{q}_{t0} being an initial (starting) point, and \mathbf{q}_{tN} being a target (final) point, where

$$\mathbf{q}_{ti} \triangleq \begin{bmatrix} \theta_{ti} \\ \mathbf{q}_{ti}^* \end{bmatrix} \in \mathbb{R}^3, \quad \mathbf{q}_{ti}^* = \begin{bmatrix} x_{ti} \\ y_{ti} \end{bmatrix} \in \mathbb{R}^2. \quad (3)$$

We assume that

$$\mathbf{q}_{t0} \triangleq \mathbf{q}(\tau = 0), \quad (4)$$

being an initial state of the system (1), and $\mathbf{q}_{tN} = [\theta_{tN} \ x_{tN} \ y_{tN}]^T$ is explicitly defined by the user. The determination of the remaining way-points \mathbf{q}_{ti} , $i = 1, \dots, N - 1$ from (2) will be described in the sequel as part of the motion planning stage. In this subsection we assume that they are given.

Next, introduce a term of the *i*-th *motion segment* denoting the motion stage associated to the transition from the \mathbf{q}_{ti-1} to the \mathbf{q}_{ti} way-point of (2). The two way-points \mathbf{q}_{ti-1} and \mathbf{q}_{ti} will be called the *boundaries* of the *i*-th motion segment. Now one can formulate the *way point following* motion task for the unicycle.

Definition 1. (*Way point following* task) Find the bounded control input functions $u_1(\cdot)$ and $u_2(\cdot)$ which take the state \mathbf{q} of the model (1) from the initial point (4) to the desired target point, \mathbf{q}_{tN} , passing according to index order through all the way-points \mathbf{q}_{ti} for $i = 1, \dots, N - 1$ with the assumed precision in sense that

$$\lim_{\tau \rightarrow \infty} \|\mathbf{q}_{tN} - \mathbf{q}(\tau)\| \leq \epsilon_N \quad (5)$$

and

$$\forall i = 1, \dots, N \quad \exists \tau_i < \infty : \quad \|\mathbf{e}_i^*(\tau_i)\| \leq \epsilon_i, \quad (6)$$

¹A similar terminology was proposed in (Lawrence *et al.*, 2008).

where

$$e_i^*(\tau) \triangleq \mathbf{q}_{ti}^* - \mathbf{q}^*(\tau) \quad (7)$$

is a position error in the i -th motion segment, and τ_i denotes the time instant when the norm $\|e_i^*(\tau)\|$ enters the assumed vicinity $\epsilon_i \geq 0$.

Note that (5) together with (6) means finite-time convergence for the target position error $e_N^*(\tau)$ to the ϵ_N -neighborhood and asymptotic convergence of the target orientation error $|\theta_{tN} - \theta(\tau)|$ to zero.

The above motion task can be accomplished in several ways. The proposition described below makes use of the specific geometrical features of the VFO stabilizer (see (Michalek and Kozłowski, 2009)), especially the so-called *directing effect*. The concept, however, involves conducting a simple motion planning stage before, which will subsequently allow smooth transition of the vehicle via motion segment boundaries. Moreover, it will be shown that the method allows free shaping of the longitudinal velocity profile $u_2 = u_2(s)$, as a function of some parameter s , in the forward as well as in the backward motion strategy. Summarizing, the presented control concept consists of two main stages: (i) the motion planning stage relying on the determination of the way-points \mathbf{q}_{ti} for $i = 1$ to $i = N - 1$, and (ii) the motion control stage accomplishing the *way point following* task formulated in Definition 1. Both stages will be described in Sections 4 and 5, respectively. To make the concept clear enough, a brief recall concerning the VFO control approach is given first in the next section (for a detailed description, see (Michalek and Kozłowski, 2009)).

3. Background on the VFO stabilizer

The form of the VFO stabilizer results from the vector field orientation control method, which originates from a simple geometrical interpretation connected with the kinematics (1). In this interpretation, the input u_1 is treated as *orienting control*, which allows one to freely change the orientation of the vector field $\mathbf{g}_2^*(\theta) = [\cos \theta \ \sin \theta]^T$ driving directly the θ variable (*orienting variable*). The second input u_2 plays the role of *pushing control*, which drives (pushes) the rest of the state variables along the current direction of $\mathbf{g}_2^*(\theta)$. The VFO stabilizer is defined by the following equations:

$$u_1(\tau) \triangleq h_1(\tau), \quad (8)$$

$$u_2(\tau) \triangleq \|\mathbf{h}^*(\tau)\| \cos \alpha(\tau), \quad (9)$$

where $\alpha = \angle(\mathbf{g}_2^*(\theta), \mathbf{h}^*)$, and the so-called *convergence vector field* $\mathbf{h} = [h_1 \ \mathbf{h}^{*T}]^T = [h_1 \ h_2 \ h_3]^T$. Here $\mathbf{h} = \mathbf{h}(\mathbf{q}_t, \mathbf{q}, \cdot) \in \mathbb{R}^3$ defines at every state point \mathbf{q} the desired convergence direction and is also a function of an instantaneous *distance* to the reference point $\mathbf{q}_t = [\theta_t \ x_t \ y_t]^T$. The particular form of this vector field is a second crucial

element of the whole VFO control strategy and in the case of the posture stabilization task it is defined as follows:

$$h_1(\tau) \triangleq k_1 e_a(\tau) + \dot{\theta}_a(\tau), \quad (10)$$

$$\mathbf{h}^*(\tau) \triangleq k_p \mathbf{e}^*(\tau) + \mathbf{v}^*(\tau), \quad (11)$$

where

$$e_a(\tau) \triangleq \theta_a(\tau) - \theta(\tau), \quad (12)$$

$$\theta_a(\tau) \triangleq \text{Atan2c}(\text{sgn}(k)h_3(\tau), \text{sgn}(k)h_2(\tau)), \quad (13)$$

$$\dot{\theta}_a(\tau) = \frac{\dot{h}_3(\tau)h_2(\tau) - \dot{h}_2(\tau)h_3(\tau)}{h_2^2(\tau) + h_3^2(\tau)}, \quad (14)$$

$$\mathbf{e}^*(\tau) \triangleq \mathbf{q}_t^* - \mathbf{q}^*(\tau), \quad \mathbf{q}_t^* = [x_t \ y_t]^T, \quad (15)$$

$$\mathbf{v}^*(\tau) \triangleq -\eta \text{sgn}(k) \|\mathbf{e}^*(\tau)\| \mathbf{g}_{2t}^*, \quad (16)$$

$$\dot{\mathbf{h}}^*(\tau) = -k_p \dot{\mathbf{q}}^*(\tau) + \dot{\mathbf{v}}^*(\tau), \quad (17)$$

$$\dot{\mathbf{v}}^*(\tau) = -\eta \text{sgn}(k) \frac{\mathbf{e}^{*T}(\tau) \dot{\mathbf{e}}^*(\tau)}{\|\mathbf{e}^*(\tau)\|} \mathbf{g}_{2t}^*, \quad (18)$$

$k_1, k_p > 0$ and $0 < \eta < k_p$ are the VFO design parameters, $\mathbf{g}_{2t}^* = [\cos \theta_t \ \sin \theta_t]^T$, and $\text{Atan2c}(\cdot, \cdot) : \mathbb{R} \times \mathbb{R} \mapsto \mathbb{R}$ is a continuous version of the four-quadrant function $\text{Atan2}(\cdot, \cdot) : \mathbb{R} \times \mathbb{R} \mapsto [-\pi, \pi]$.

Equations (8) to (18) reveal the VFO control strategy. Equation (13) defines the desired auxiliary orientation angle, expected to be followed by the vehicle, and computed according to the current direction of \mathbf{h}^* . The additional term $\text{sgn}(k) \in \{+1, -1\}$ can be treated here as a decision variable, which allows choosing the desired motion strategy (forward/backward) of the vehicle along the direction of \mathbf{h}^* . According to (12), (10) and (8), the orienting control u_1 is responsible for reorienting the vehicle to make the auxiliary orientation error (12) tend to zero. A geometrical interpretation of the above follows: setting $e_a = 0$ is equivalent to making the direction (and the orientation if $\text{sgn}(k) = +1$) of $\mathbf{g}_2^*(\theta)$ coincident with the direction determined by \mathbf{h}^* . In addition, with appropriate value selection for $\text{sgn}(k)$ and the input u_2 , it consequently implies that the longitudinal velocity vector $\dot{\mathbf{q}}^*$ can be aligned with the convergence vector \mathbf{h}^* and the vehicle position can be driven to the reference point.

It is worth noting that the definition of \mathbf{h}^* proposed in (11) is peculiar in the sense that at the limit for $\mathbf{e}^* \rightarrow \mathbf{0}$ the auxiliary variable (13) converges to the reference orientation θ_t . This has a great importance for the convergence of the vehicle orientation to the reference one in a neighborhood of the reference position \mathbf{q}_t^* . The pushing control u_2 proposed in (9) drives the substate vector \mathbf{q}^* along the current direction of $\mathbf{g}_2^*(\theta)$ with the intensity proportional to the current orthogonal projection of \mathbf{h}^* onto $\mathbf{g}_2^*(\theta)$ realizing the so-called *careful pushing* strategy (Michalek and Kozłowski, 2009).

Summarizing, the control inputs of the VFO approach are designed in a way which guarantees that the

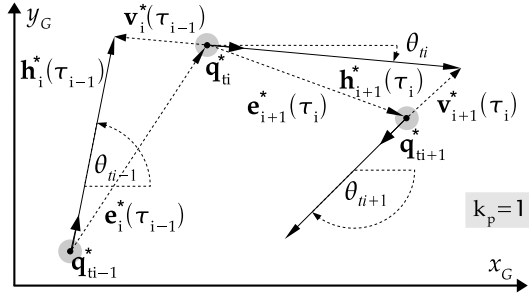


Fig. 3. Description of particular vectors and the explanation of way-point orientation determination in subsequent motion segments for the VFO motion planning strategy (h^* denoted for $k_p = 1$ and $\text{sgnU}2_i = +1$).

chosen by the user. The terms in the above equations play in the i -th segment the same role as described in Section 3. The decision variable $\text{sgnU}2_i$ (introduced here instead of the $\text{sgn}(k)$ function from (13)–(18)) allows choosing the motion strategy during approaching the i -th way-point ($\text{sgnU}2_i = +1$ for forward, $\text{sgnU}2_i = -1$ for backward motion).

The definitions (19)–(22) were written as functions of time, since they will be time-dependent during the motion realization stage. However, for the planning procedure, only their values at the initial time instant τ_{i-1} are important, since at this time instant the vehicle should arrive at the beginning of the i -th motion segment. Hence, for $\tau = \tau_{i-1}$, the auxiliary angle (22) takes the value

$$\theta_{ai}(\tau_{i-1}) = \arg(\mathbf{h}_i^*(\tau_{i-1})), \quad (24)$$

where for simplicity we introduced the notion $\arg(\mathbf{h}^*) \equiv \text{Atan2c}(\text{sgnU}2_i \cdot h_3, \text{sgnU}2_i \cdot h_2)$. According to the VFO motion planning principle mentioned before, the desired orientation of the way-point \mathbf{q}_{ti-1}^* results from the following substitution:

$$\theta_{ti-1} := \theta_{ai}(\tau_{i-1}). \quad (25)$$

Note that for the nominal case one has $e_i^*(\tau_{i-1}) \equiv \mathbf{q}_{ti}^* - \mathbf{q}_{ti-1}^*$. Equation (25) expresses the VFO motion planning strategy. It means that the desired orientation in the i -th way-point should be consistent with the orientation of the convergence vector \mathbf{h}^* computed for the point \mathbf{q}_{ti}^* defining simultaneously the convergence direction to the next way-point from the set (2).

The VFO motion planning strategy is graphically explained in Fig. 3. The following algorithm summarizes the computations involved in the VFO motion planning stage:

- S0. Initial data: $\mathbf{q}_{t0} \equiv \mathbf{q}(0)$, \mathbf{q}_{tN} , $k_p > 0$
and \mathbf{q}_{ti}^* , η_i , $\text{sgnU}2_i$ for all $i = 1, \dots, N$;
- S1. Counter initialization: $i := N$;
- S2. $e_i^*(\tau_{i-1}) = \mathbf{q}_{ti}^* - \mathbf{q}_{ti-1}^*$;

$$\text{S3. } \mathbf{v}_i^*(\tau_{i-1}) = -\eta_i \text{sgnU}2_i \|e_i^*(\tau_{i-1})\| \mathbf{g}_{2ti}^*;$$

$$\text{S4. } \mathbf{h}_i^*(\tau_{i-1}) = k_p e_i^*(\tau_{i-1}) + \mathbf{v}_i^*(\tau_{i-1});$$

$$\text{S5. } \theta_{ai}(\tau_{i-1}) = \arg(\mathbf{h}_i^*(\tau_{i-1}));$$

$$\text{S6. } \theta_{ti-1} := \theta_{ai}(\tau_{i-1});$$

$$\text{S7. IF } (i == 2) \text{ THEN STOP} \\ \text{ELSE } i := i - 1 \text{ and GOTO S2.}$$

5. VFO control for way point following

After the motion planning procedure, the second stage of the proposed concept, namely, motion realization, is considered. We propose to utilize at this stage the modified version of the VFO feedback controller presented in Section 3. This modification results from the following important issues. First, the original VFO stabilizer (8)–(9) is defined only for one motion segment determined by the initial and the final posture, guaranteeing asymptotic convergence for the posture error to zero. This means that the final position cannot be reached in finite time. Second, longitudinal velocity of the vehicle controlled by the original pushing control (9) evolves from relatively high value at the beginning of the transient stage to zero in the final stage. Hence, using the original definition of the controller for the *way point following* task would prevent the vehicle from passing smoothly and in finite time through particular segment boundaries and, as a consequence, from accomplishing the task considered.

According to the above, we propose to organize the motion realization stage as follows. To guarantee reaching the segment boundary in finite time, let us replace the asymptotic convergence demand of the original VFO stabilizer with practical convergence to the assumed non-zero vicinities $\epsilon_1, \dots, \epsilon_N > 0$ of the way-points $\mathbf{q}_{t1}, \dots, \mathbf{q}_{tN}$ in the particular motion segments. Relaxing the convergence demand remains consistent with Definition 1 and seems to be practically justified. We also propose, following the works of (Sasiadek and Duleba, 1995) and (Sordalen and de Wit, 1993), the switching procedure, which will be responsible for the activation of the next way-point from the set \mathcal{S}_t as soon as the position error norm determined for the i -th motion segment reaches the assumed ϵ_i -neighborhood of the i -th way-point. Activating the way-point should be understood as passing it on to the realization stage. The switching procedure can be described by the increasing condition for the index i which indicates the currently active, i.e., being realized, motion segment:

$$\text{IF } (\|e_i^*\| \leq \epsilon_i) \text{ AND } (i < N) \text{ THEN } i := i + 1, \quad (26)$$

assuming additionally that the initial index value $i := 1$ is set for $\tau = 0$ (beginning of the motion realization stage).

Let us now define the VFO control inputs for the *way point following* task. The modified pushing control input for particular motion segments is defined as follows:

$$u_2(\tau) \triangleq \begin{cases} \rho_i \|\mathbf{h}_i^*(\tau)\| \cos \alpha_i(\tau) & \text{for } \tau \in [\tau_{i-1}, \tau_i), \\ 0 & \text{for } \tau \geq \tau_N, \end{cases} \quad (27)$$

where $i = 1, \dots, N$, $\mathbf{h}_i^*(\tau)$ is defined in (21), $\alpha_i(\tau) = \angle(\mathbf{g}_2^*(\theta(\tau)), \mathbf{h}_i^*(\tau))$, and the non-negative continuous scaling function $\rho_i = \rho_i(\cdot)$ is introduced in order to properly shape the longitudinal velocity profile along the motion segments. To make our discussion more general, we do not determine here any particular form of the function ρ_i . However, an example will be given in Subsection 5.1. The definition (27) indicates that the vehicle is stopped after reaching the assumed neighborhood $\epsilon_N > 0$ of the target point \mathbf{q}_{tN} . In this way, the motion time horizon in the realization stage is finite, as required in Definition 1.

The orienting control is defined as follows:

$$u_1(\tau) \triangleq \begin{cases} k_1 e_{ai}(\tau) + \dot{\theta}_{ai}(\tau) & \text{for } \tau \in [\tau_{i-1}, \tau_i), \\ k_1(\theta_{tN} - \theta(\tau)) & \text{for } \tau \geq \tau_N, \end{cases} \quad (28)$$

where $i = 1, \dots, N$, $k_1 > 0$ is a design coefficient, and $e_{ai}(\tau) = \theta_{ai}(\tau) - \theta(\tau)$ with $\theta_{ai}(\tau)$ defined in (22). The feed-forward term $\dot{\theta}_{ai}$ comes from time-differentiation of (22) and has the form

$$\dot{\theta}_{ai}(\tau) = \frac{\dot{h}_{3i}(\tau)h_{2i}(\tau) - \dot{h}_{2i}(\tau)h_{3i}(\tau)}{h_{2i}^2(\tau) + h_{3i}^2(\tau)}, \quad (29)$$

with $\mathbf{h}_i^*(\tau) = [h_{2i}(\tau) \ h_{3i}(\tau)]^T$ defined by (20)–(21) and with

$$\dot{\mathbf{h}}_i^*(\tau) = -k_p \dot{\mathbf{q}}^*(\tau) + \dot{\mathbf{v}}_i^*(\tau) \quad (30)$$

(compare (17)), where

$$\dot{\mathbf{v}}_i^*(\tau) = -\eta_i \operatorname{sgn} U_2 \frac{\mathbf{e}_i^{*T}(\tau) \dot{\mathbf{e}}_i^*(\tau)}{\|\mathbf{e}_i^*(\tau)\|} \mathbf{g}_{2ti}^*, \quad (31)$$

with \mathbf{g}_{2ti}^* determined in (23), comes from time-differentiation of (20).

Comparing (28) and (8), one can find that for all N motion segments the orienting control for the *way point following* task is almost analogous to the original definition for the VFO stabilizer. The difference comes from the switching procedure applied here and from the last stage (for $\tau \geq \tau_N$), where the modified orienting control has to stabilize the orientation of the vehicle stopped by the pushing control (27) in the assumed non-zero neighborhood ϵ_N of the target point \mathbf{q}_{tN} .

Remark 1. The definitions (22) and (29) are well defined for $\|\mathbf{h}_i^*\| \neq 0$. Since the condition $\|\mathbf{h}_i^*\| = 0$ can be met only for $\|\mathbf{e}_i^*\| = 0$ (see (21) and (20)), one avoids this indeterminacy assuming that all vicinities $\epsilon_1, \dots, \epsilon_N$ for the way-points are greater than zero. This implies that the

vehicle never reaches the current i -th way-point before the switching procedure activates the next way-point from the set \mathcal{S}_t , or before the pushing input (27) stops the vehicle (for $\tau \geq \tau_N$) in the neighborhood ϵ_N of the target point \mathbf{q}_{tN} .

The control input definitions (27) and (28) are proposed as a result of some heuristic approach based on the authors' experiences obtained so far during simulation and experimental tests with VFO controllers (see (Michałek and Kozłowski, 2009)). Stability and error convergence analysis in the closed-loop system with the proposed VFO controller for the *way point following* task is conducted in Subsection 5.2.

5.1. Remarks on scaling function selection. The scaling function ρ introduced in the definition (27) can be selected in many ways according to a particular application. The only constraint of its construction lies in positive semi-definiteness. The possible selection determines $\rho = \rho(s)$ as a function of some independent and normalized parameter $s \in [0, 1]$. In a particular case, s can be a time variable ($s \triangleq \tau$). However, this selection would lead to the *points-tracking* task rather than to *way point following*, considered in this paper. For the latter, it seems to be more appropriate to define s in terms of some geometrical terms related to a realized motion task (with analogy to the well-known proposition from (Samson, 1992)). One such proposition for the i -th motion segment can be defined as follows:

$$s_i \triangleq 1 - \frac{\|\mathbf{h}_i^*(\tau)\|}{\|\mathbf{h}_i^*(\tau_{i-1})\|}, \quad (32)$$

where $\tau \in [\tau_{i-1}, \tau_i]$.

Since $\|\mathbf{h}_i^*(\tau)\|$ can evolve in time only when the vehicle moves with a non-zero longitudinal velocity u_2 , the parameter s_i evolves also in relation to vehicle motion. Now, the function $\rho_i = \rho_i(s_i)$ allows shaping longitudinal velocity taking, for instance,

$$\rho_i(s_i) \triangleq \frac{\bar{\rho}_i(s_i)}{\|\mathbf{h}_i^*(\tau)\|}, \quad (33)$$

where $\bar{\rho}_i(s_i)$ is a design function founded, for example, on the polynomial basis. The simplest example is the zero-order polynomial $\bar{\rho}_i \triangleq U_2$ with $U_2 > 0$ being a constant denoting the desired driving velocity of the controlled vehicle⁵. Substituting (33) with the mentioned zero-order polynomial into the definition (27) gives the particular form of the VFO pushing control in the i -th motion segment as follows:

$$u_2(\tau) = U_2 \cos \alpha_i(\tau). \quad (34)$$

Note that the above proposition generally results in a piecewise continuous input signal, with the possible dis-

⁵Understood as an absolute value.

continuity points only in transition through the motion segment boundaries (at the time instants τ_i).

5.2. Stability and convergence analysis. It will be shown that the VFO feedback controller defined in (27) and (28) applied to the vehicle model (1) together with the motion segment switching condition (26) guarantees accomplishing the task given in Definition 1. More specifically, one can show that

A1. The vehicle position error $\|e_i^*(\tau)\|$ in any i -th motion segment converges to the assumed non-zero ϵ_i -neighborhood of the i -th way-point position q_{ti}^* in finite time. As a consequence, the vehicle position converges from the initial point $q^*(0)$ to the target one q_{tN}^* in finite time as well.

A2. The vehicle orientation $\theta(\tau)$ exponentially converges to the auxiliary orientation $\theta_{ai}(\tau)$ in any i -th motion segment.

A3. The vehicle orientation $\theta(\tau)$ asymptotically converges to the target orientation θ_{tN} after the vehicle reaches the assumed vicinity ϵ_N of the target position q_{tN}^* .

Let us consider the i -th motion segment joining the current vehicle state $q(\tau)$ with the i -th way-point q_{ti}^* . The analysis starts by applying the orienting input (28) into (1), which gives

$$\dot{e}_{ai}(\tau) + k_1 e_{ai}(\tau) = 0 \quad \Rightarrow \quad \lim_{\tau \rightarrow \infty} e_{ai}(\tau) = 0. \quad (35)$$

The above equation allows concluding A2.

In the next step, let us recall the definition (7), which implies $\dot{e}_i^* = -\dot{q}^*$. This relation can be equivalently rewritten as (cf. (21))

$$\dot{e}_i^* = -\dot{q}^* + \rho_i(\mathbf{h}_i^* - k_p e_i^* - \mathbf{v}_i^*),$$

where ρ_i is the scaling function from (27). After reordering the above equation, one obtains

$$\dot{e}_i^* + \rho_i k_p e_i^* = \rho_i \mathbf{r}_i - \rho_i \mathbf{v}_i^*, \quad (36)$$

where

$$\mathbf{r}_i = \mathbf{h}_i^* - \mathbf{g}_2^*(\theta) \bar{u}_2 \quad \text{with} \quad \bar{u}_2 := \|\mathbf{h}_i^*\| \cos \alpha_i. \quad (37)$$

The latter formula can be easily obtained recalling that $\dot{q}^* = \mathbf{g}_2^*(\theta) u_2$, where $\mathbf{g}_2^* = [\cos \theta \ \sin \theta]^T$ (see (1) and (27)): $\dot{q}^* = \mathbf{g}_2^*(\theta) \rho_i \|\mathbf{h}_i^*\| \cos \alpha_i = \rho_i \mathbf{g}_2^*(\theta) \bar{u}_2$. Additionally, it can be shown (see Appendix) that the following two relations hold:

$$\|\mathbf{r}_i\| = \|\mathbf{h}_i^*\| \gamma_i(\theta), \quad \lim_{\theta \rightarrow \theta_{ai}} \gamma_i(\theta) = 0, \quad (38)$$

where $\gamma_i(\theta) = \sqrt{1 - \cos^2 \alpha_i(\theta)} \in [0, 1]$ and $\alpha_i(\theta) = \angle(\mathbf{g}_2^*(\theta), \mathbf{h}_i^*)$. Let us introduce the positive definite function $V_i(e_i^*) \triangleq \frac{1}{2} e_i^{*T} e_i^*$. Its time-derivative along the solution of (36) can be estimated as follows:

$$\begin{aligned} \dot{V}_i &= e_i^{*T} \dot{e}_i^* = e_i^{*T} [-\rho_i k_p e_i^* + \rho_i \mathbf{r}_i - \rho_i \mathbf{v}_i^*] \\ &= -\rho_i k_p \|e_i^*\|^2 + \rho_i e_i^{*T} \mathbf{r}_i - \rho_i e_i^{*T} \mathbf{v}_i^* \\ &\leq -\rho_i \left[k_p \|e_i^*\|^2 - \|e_i^*\| \|\mathbf{r}_i\| - \|e_i^*\| \|\mathbf{v}_i^*\| \right] \\ &\stackrel{(20,38)}{=} -\rho_i \left[k_p \|e_i^*\|^2 - \|e_i^*\| \|\mathbf{h}_i^*\| \gamma_i - \eta_i \|e_i^*\|^2 \right] \\ &= -\rho_i \left[(k_p - \eta_i) \|e_i^*\|^2 - \gamma_i \|e_i^*\| \|k_p e_i^* + \mathbf{v}_i^*\| \right] \\ &\leq -\rho_i \left[(k_p - \eta_i - \gamma_i k_p) \|e_i^*\|^2 - \gamma_i \|e_i^*\| \|\mathbf{v}_i^*\| \right] \\ &\stackrel{(20)}{=} -\rho_i \left[(k_p - \eta_i - \gamma_i k_p) \|e_i^*\|^2 - \gamma_i \eta_i \|e_i^*\|^2 \right] \\ &= -\rho_i [k_p - \eta_i - \gamma_i (k_p + \eta_i)] \|e_i^*\|^2 \\ &= -\rho_i \zeta(\gamma_i) \|e_i^*\|^2. \end{aligned}$$

The above time-derivative is negative definite for the positive function ρ_i if $\zeta(\gamma_i(\tau)) > 0$. The last condition will be analyzed in the sequel, but first we focus our attention on the function ρ_i , which has crucial influence on the rate of position error time-evolution. Recalling Subsection 5.1, let us define ρ_i as follows:

$$\rho_i \triangleq \frac{U_2}{\|\mathbf{h}_i^*(\tau)\|}, \quad (39)$$

where $U_2 > 0$ determines the user-defined longitudinal velocity value along the i -th motion segment. Using the definition (21), one gets $\|\mathbf{h}_i^*(\tau)\| = \|e_i^*(\tau)\| \cdot \|\boldsymbol{\vartheta}_i(\tau)\|$, where $\boldsymbol{\vartheta}_i(\tau) = k_p \boldsymbol{\vartheta}_{ei}(\tau) - \eta_i \text{sgn} U_2 \mathbf{g}_{2ti}^*$ and $\boldsymbol{\vartheta}_{ei}(\tau)$ is a unit vector of the position error $e_i^*(\tau)$. Note that, since $\eta_i < k_p$, it is guaranteed that $\|\boldsymbol{\vartheta}_i(\tau)\| \neq 0$ for all $\tau \geq 0$. Now, an upper bound of \dot{V}_i can be calculated as follows:

$$\dot{V}_i \leq -\frac{U_2 \cdot \zeta(\gamma_i)}{\|\mathbf{h}_i^*(\tau)\|} \|e_i^*\|^2 = -\frac{U_2 \cdot \zeta(\gamma_i)}{\|\boldsymbol{\vartheta}_i(\tau)\|} \|e_i^*\|.$$

Let us recall and analyze the inequality $\zeta(\gamma_i(\tau)) > 0$, which still remains the sufficient condition for the convergence of $\|e_i^*\|$. The convergence condition takes the following form:

$$\zeta(\gamma_i(\tau)) > 0 \quad \Leftrightarrow \quad \gamma_i(\tau) < \frac{k_p - \eta_i}{k_p + \eta_i}. \quad (40)$$

By assumption, one has $\forall_{i=1, \dots, N} 0 < \eta_i < k_p$, hence the ratio $(k_p - \eta_i)/(k_p + \eta_i) < 1$. Since $\gamma_i(\theta(\tau)) \in [0, 1]$ for all $\tau \in \mathbb{R}$, and since (35) and (38) hold, one concludes that there exists a finite time instant $\tau_{\gamma_i} \in [\tau_{i-1}, \infty)$ such that

$$\forall_{\tau \geq \tau_{\gamma_i}} \quad \gamma_i(\tau) < \frac{k_p - \eta_i}{k_p + \eta_i}, \quad (41)$$

and the function $\zeta(\gamma_i(\tau))$ becomes positive for all $\tau \geq \tau_{\gamma_i}$. For the finite time-interval $[\tau_{i-1}, \tau_{\gamma_i}]$ we cannot, in general, guarantee that $\zeta(\gamma_i(\tau))$ is positive and, consequently, that V_i is non-increasing. However, we can show that the finite-time escape for $\|e_i^*\|$ is also not possible. Namely, in the worst case when $\gamma_i = 1$ one obtains $\zeta(\gamma_i = 1) = -2\eta_i$ yielding $\dot{V}_i(\tau) \leq (2U_2\eta_i \|e_i^*(\tau)\| / \|\vartheta_i(\tau)\|) < \infty$ (we assume that $\|e_i^*(0)\| < \infty$). Since the last inequality may hold only for $\tau \in [\tau_{i-1}, \tau_{\gamma_i}]$, where τ_{γ_i} is finite, the norm $\|e_i^*\|$, the functions V_i and \dot{V}_i remain bounded also in the time interval $[\tau_{i-1}, \tau_{\gamma_i}]$. Hence, let us consider time-evolution of $V_i(\tau)$ and $\|e_i^*(\tau)\|$ for $\tau \geq \tau_{\gamma_i}$, accepting that $V_i(e_i^*(\tau_{\gamma_i})) \geq V_i(e_i^*(0))$.

Now, an upper bound of the time-derivative of the function V_i can be estimated as follows:

$$\dot{V}_i \leq -\frac{U_2 \cdot \zeta(\gamma_i)}{\|\vartheta_i(\tau)\|} \|e_i^*\| \leq -c_i \sqrt{V_i}, \quad (42)$$

with

$$c_i = \frac{\sqrt{2}U_2\zeta(\gamma_{im})}{k_p + \eta_i} = \sqrt{2}U_2 \left(\frac{k_p - \eta_i}{k_p + \eta_i} - \gamma_{im} \right) > 0. \quad (43)$$

The bounding value γ_{im} from (43) can be estimated in two ways:

W1. as the initial value $\gamma_i(\tau_{i-1})$ if it fulfills the condition (40) at the beginning of the i -th motion segment ($\tau_{\gamma_i} = \tau_{i-1}$), otherwise

W2. as a maximal value of function γ_i which fulfills (40), i.e., equal to $\gamma_i(\tau_{\gamma_i})$.

According to the work of (Bhat and Bernstein, 2000), the result obtained in (42) allows concluding finite-time convergence for the position error $e_i^*(\tau)$ to zero in the i -th motion segment. The convergence time interval $T_i = \tau_i - \tau_{\gamma_i}$ can be estimated as follows, cf. (Bhat and Bernstein, 2000)

$$T_i \leq \hat{T}_i, \quad \text{where} \quad \hat{T}_i = \frac{2}{c_i} \sqrt{V_i(e_i^*(\tau_{\gamma_i}))}. \quad (44)$$

Note that \hat{T}_i depends on the coefficient c_i estimated in (43), which in turn depends on the estimated value of γ_{im} . When γ_{im} can be estimated as in W1, (44) may be useful in practice, as will be shown in Section 6. In the case of W2, however, (44) gives rather a theoretical solution, since it provides a very conservative estimate of the convergence time.

As a direct consequence of the finite-time convergence result, the time instant τ_i when the norm $\|e_i^*(\tau)\|$ enters into the nonzero ϵ_i -neighborhood of the i -th way-point must be finite and is less than $\tau_{\gamma_i} + \hat{T}_i$. Using the

switching procedure (26), which activates the next way-point in the time instant τ_i , implies that the N motion segments are completed in finite time:

$$\tau_N < \sum_{i=1}^N ((\tau_{\gamma_i} - \tau_{i-1}) + \hat{T}_i) \quad \text{with} \quad \tau_0 = 0.$$

Since the input $u_2(\tau)$ is zero for $\tau \geq \tau_N$ (compare (27)), the vehicle stops in the ϵ_N -neighborhood of the target position q_{tN}^* . This completes A1.

To show A3, it suffices to substitute into the model (1) the orienting control input (28) for $\tau \geq \tau_N$ resulting in the following equation: $\dot{\theta}(\tau) + k_1\theta(\tau) = k_1\theta_{tN}$. It is evident that, after reaching the ϵ_N -neighborhood of the target position, the vehicle orientation will converge exponentially to the target orientation θ_{tN} with the time constant equal to $1/k_1$.

Next it is of interest to discuss two issues not treated explicitly in the preceding analysis and concerning control quality in the closed-loop system with the proposed VFO controller.

First, it is worth noting that the function ρ_i introduced in (27) can take the zero value in a finite number of time instants not violating at the same time the finite-time convergence result obtained above for the position error $e_i^*(\tau)$. It can be seen from (36) that for $\rho_i = 0$ one has $\dot{e}_i^* = \mathbf{0}$ and the position error cannot diverge. This property gives great flexibility in shaping, using the function ρ_i , the longitudinal velocity profile for the vehicle in practical tasks. The second issue concerns time evolution of the vehicle orientation $\theta(\tau)$ in relation to the way-point orientations θ_{ti} computed in the planning stage for $i = 1, \dots, N - 1$. According to the motion planning procedure presented in Section 4, the way-point orientation θ_{ti} is computed to keep the continuity in time evolution of the auxiliary angle $\theta_{ai}(\tau)$ (defined in (22)) during segment boundary transition in the motion realization stage.

The continuity issue can be explained as follows. For the case in which we assume that for all $i = 1, \dots, N - 1$ $\lim_{\tau \rightarrow \tau_i} \|e_i^*(\tau)\| = 0$ and $e_{ai}(\tau) \equiv 0 \Rightarrow \theta(\tau) \equiv \theta_{ai}(\tau)$, one can show that $\lim_{\tau \rightarrow \tau_i} \theta_{ai}(\tau) = \theta_{ti}$. Since $\theta_{ti} := \theta_{ai+1}(\tau_i)$ (according to the step S6 in Section 4), one concludes that $\lim_{\tau \rightarrow \tau_i} \theta_{ai}(\tau) = \theta_{ai+1}(\tau_i)$ and, as a consequence of the assumed equality $\theta(\tau) \equiv \theta_{ai}(\tau)$, that $\theta(\tau_i^-) = \theta(\tau_i^+)$, yielding continuous evolution also for the vehicle orientation during the segment boundary transition. However, due to the assumption about the non-zero ϵ_i values in the motion realization stage, one cannot generally guarantee that the auxiliary orientation variable $\theta_{ai}(\tau)$ (and also the vehicle orientation $\theta(\tau)$) will precisely converge to the planned way-point orientation θ_{ti} in the neighborhood of the segment boundary. The resultant discontinuity in the evolution of the auxiliary variable can be minimized by increasing the intensity of the *direct-*

ing effect, choosing higher values for the η_i parameters⁶, as mentioned in Section 3. It is worth noting that, in spite of mentioned discontinuity, the feed-forward term $\hat{\theta}_{ai}(\tau)$ present in (28) and computed according to (29) will be bounded, since the time-derivatives (30) and (31) are also bounded during the segment boundary transition for any non-zero value of ϵ_i .

6. Simulation results

To show the effectiveness of the proposed concept, two numerical simulation tests, denoted as SimA and SimB, are conducted for the unicycle model (1). In both cases the same set of the six way-points is defined with the position components $[x_{ti} \ y_{ti}]^T = \mathbf{q}_{ti}^*$ presented in Tables 1 and 2. The initial vehicle posture, being simultaneously the first way-point, is chosen as: $\mathbf{q}_{t0} = \mathbf{q}(0) = [0 \ -4 \ 3.5]^T$. The VFO parameters for all $i = 1, \dots, N$ are $\eta_i = 3.5$, $\epsilon_i = 0.005$ m, $k_1 = 10$, and $k_p = 5$ (both in [1/s])⁷. Tables 1 and 2 include also the way-point orientations θ_{ti} . The orientations computed in the motion planning stage are denoted in bold. The initial and the target way-point orientations (θ_{t0} and θ_{tN}) are defined in advance by the user and are not modified during the planning stage. For the simulations, the scaling function ρ in the definition (27) is chosen as follows:

$$\rho_i(\mathbf{h}_i^*) \triangleq \begin{cases} \frac{U_2}{\|\mathbf{h}_i^*(\tau)\|} & \text{for } i = 1, \dots, N-1, \\ \frac{U_2}{\|\mathbf{h}_N^*(\tau_{N-1})\|} & \text{for } i = N, \end{cases} \quad (45)$$

with $U_2 = 0.4$ m/s.

Note that for all the motion segments except the last one (the N -th one) the scaling function ρ_i has the same form as in (39), which was used in the convergence analysis in Subsection 5.2 leading to the finite-time convergence result. The proposed definition of ρ_N has been motivated only by the requirement of smooth decreasing of longitudinal vehicle velocity during approaching the ϵ_N -neighborhood of the target position \mathbf{q}_N^* . Since in this case the Lyapunov analysis yields the inequality $\dot{V}_N \leq -(U_2\zeta(\gamma_N)/\|\mathbf{h}_N^*(\tau_{N-1})\|)\|\mathbf{e}_N^*\|^2$, the convergence of the position error to zero is asymptotic. However, since the ϵ_N -neighborhood is greater than zero (by assumption), the entering-time instant τ_N must be finite also in this case.

Using the definition (45) in (27) gives the pushing control input in the form of (34) for all the motion segments excluding the last one. In the N -th motion segment,

the pushing input takes the form

$$u_2 = U_2 \frac{\|\mathbf{h}_N^*(\tau)\|}{\|\mathbf{h}_N^*(\tau_{N-1})\|} \cos \alpha_N(\tau),$$

which continuously converges to zero when the vehicle approaches the ϵ_N -neighborhood of the target way-point position.

The simulation tests SimA and SimB differ only in motion strategy selection indicated by the values of the $\text{sgn}U_2$ parameter ($\text{sgn}U_2 = +1$ for the forward motion and $\text{sgn}U_2 = -1$ for the backward one) included in Tables 1 and 2. According to the presented values, the desired vehicle motion in the test SimA was set to the forward strategy for all motion segments. In the test SimB, the way-points \mathbf{q}_{t2} and \mathbf{q}_{t3} should be approached in the backward manner. The obtained results⁸ are illustrated in Figs. 4–7. The way-point positions are indicated in Figs. 4 and 5 by small circles; the way-point orientations are denoted by short straight lines.

It is worth noting, referring to Figs. 6 and 7, that time evolution of the posture errors $e_{\theta i}(\tau) = \theta_{ti} - \theta(\tau)$, $e_{xi}(\tau) = x_{ti} - x(\tau)$, and $e_{yi}(\tau) = y_{ti} - y(\tau)$ is fast and non-oscillatory towards the subsequent way-points. From the time plots on a logarithmic scale one can see that the evolution rate of errors in the first four motion segments is higher than exponential, as a consequence of finite-time convergence. Tables 3 and 4 present the estimated and the obtained time intervals for the three selected way-points in both simulation tests. The comparison of particular values reveals that the upper bound from (44) computed for the coefficient estimated in (43) is rather conservative in the cases considered. The task realization times τ_N for particular tests are $\tau_N = 39.6$ s for SimA and $\tau_N = 39.8$ s for SimB.

The plots in Figs. 4 and 5 indicate that vehicle behavior along the particular segments seems to be intuitively predictable in spite of the fact that the path between the way-points is not defined explicitly. Note also that time evolution of the auxiliary variable $\theta_{ai}(\tau)$ does not reveal any substantial discontinuity (caused by the non-zero ϵ_i vicinities), which, together with the characteristic *directing effect*, yields practically acceptable and smooth transition through the motion segment boundaries. Worth noting is the simplicity in motion strategy selection (forward/backward) involving only the appropriate value selection for the decision variable $\text{sgn}U_2$.

7. Conclusions

The VFO motion planning and feedback control strategy presented in this paper allows treating the problem of driving the unicycle through the sequence of desired way-

⁶In relation to the chosen value of the k_p coefficient (see (Michalek and Kozłowski, 2009)).

⁷Particular values have been selected here according to the general hints presented in (Michalek and Kozłowski, 2009) and in part by the trial-and-error method.

⁸Simulations were conducted with the Matlab/Simulink software using the variable-step ode45 (Dormand-Prince) solver option.

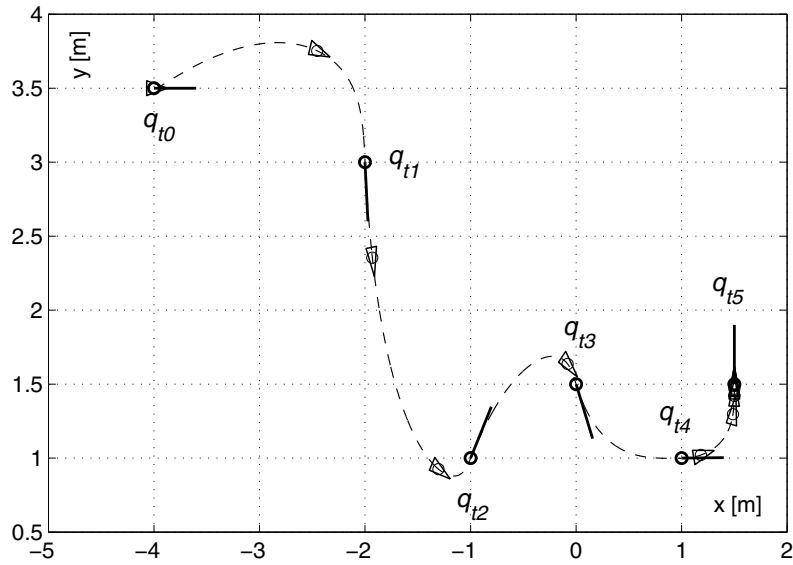


Fig. 4. SimA: vehicle motion in the global frame obtained in the simulation A.

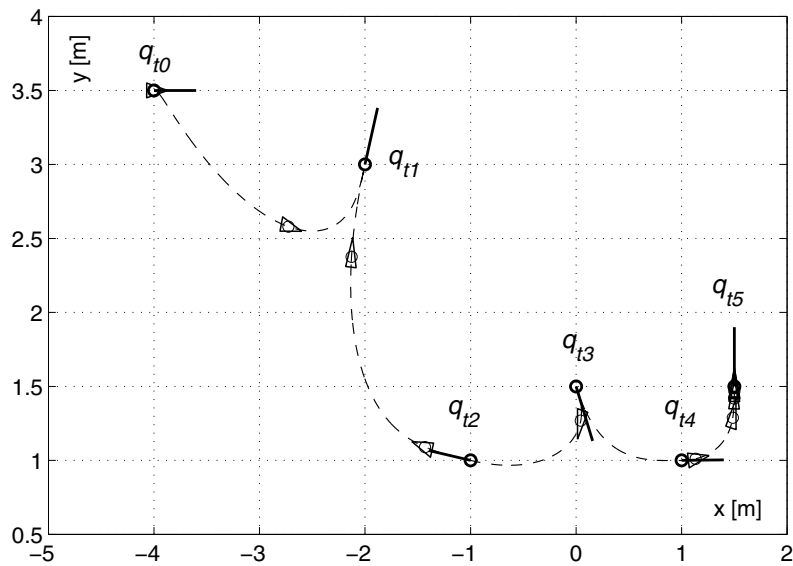


Fig. 5. SimB: vehicle motion in the global frame obtained in the simulation B.

Table 1. Coordinates of the way-points and motion strategy used in the simulation A.

i	0	1	2	3	4	5
θ_{ti} [rad]	0.00	-1.50	1.05	-1.17	0.01	1.57
x_{ti} [m]	-4.0	-2.0	-1.0	0.0	1.0	1.5
y_{ti} [m]	3.5	3.0	1.0	1.5	1.0	1.5
$\text{sgn}U2_i$	-	+1	+1	+1	+1	+1

Table 2. Coordinates of the way-points and motion strategy used in the simulation B.

i	0	1	2	3	4	5
θ_{ti} [rad]	0.00	-5.02	-3.31	-1.17	0.01	1.57
x_{ti} [m]	-4.0	-2.0	-1.0	0.0	1.0	1.5
y_{ti} [m]	3.5	3.0	1.0	1.5	1.0	1.5
$\text{sgn}U2_i$	-	+1	-1	-1	+1	+1

points in a simplified and effective way. The simplification results from the fact that the motion planning stage does not involve any interpolating procedure between the

way-points with any geometrical path as opposed to many solutions proposed in the literature. Motion planning relies only on way-point orientation computations starting

Table 3. Selected values of the obtained and the estimated convergence time intervals for the test SimA.

i	2	3	4
T_i [s]	6.5	3.5	3.0
\hat{T}_i [s]	31.8	15.9	16.3
τ_i [s]	12.9	16.4	19.4

Table 4. Selected values of the obtained and the estimated convergence time intervals for test SimB.

i	2	3	4
T_i [s]	6.7	3.5	3.0
\hat{T}_i [s]	31.8	16.0	16.1
τ_i [s]	13.1	16.6	19.6

from the target posture and finishing on the first user-defined way-point from the set \mathcal{S}_t . The simplicity of the approach comes from the unique features of the VFO stabilizer which was adapted here to the *way point following* task. The main important features include predictable and non-oscillatory transients of the vehicle with the useful *directing effect*, intuitive geometrical interpretation of VFO control inputs and, as a consequence, very simple parametric synthesis of the controller. The concept guarantees passing in finite time from the initial vehicle posture to the target one driving via all the way-points with the assumed finite precision, yielding finally *practical stability* of the closed-loop system⁹ in the neighborhood of the target point. The desired motion strategy (forward/backward motion) in approaching the particular way-points can be freely and easily shaped by the bi-valued decision variable (in our case, $\text{sgn}U_{2_i}$). The profile of longitudinal vehicle velocity can be easily shaped by introducing the scaling function in definition of the pushing input. The predictability of vehicle motion during transients between particular way-points together with the flexibility of motion strategy shaping allows designing the resulting vehicle path geometry in a simple and effective way.

Possible future extensions of the work may include automatic selection of the η_i parameters responsible for the intensity of the directing effect, automatic motion safety estimation in the sense of the room size needed for task realization, and the adoption of the proposed concept to other classes of mobile robots. Experimental validation of the proposed method will be conducted in near future using a newly designed differentially-driven *Leonardi* transportation vehicle, being now under construction. The control system will be designed in a cascade form with two low-level PI velocity control loops for vehicle direct-drives. The higher-level kinematic VFO controller pro-

⁹Practical stability means ultimate boundedness of the stabilization error by its convergence to the assumed vicinity of the origin (Morin and Samson, 2003; Kozłowski and Pazderski, 2004).

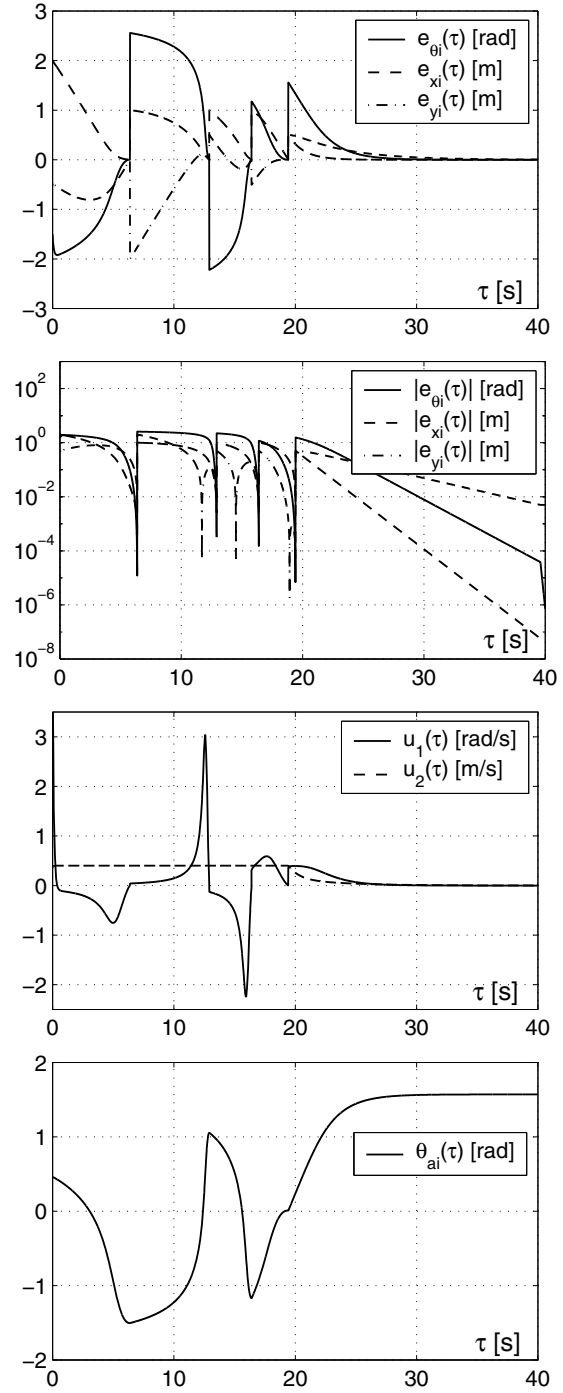


Fig. 6. SimA: time plots of signals obtained in the simulation A.

posed in this paper will be responsible for computing the desired wheel velocities for the low-level PI loops. Position feedback of the vehicle platform layer will be realized by the fusion of signals from wheel encoders, a laser scanner and a vision system mounted on board. Practical utilization of the proposed control method involves treating the control inputs limitations, which can be taken into ac-

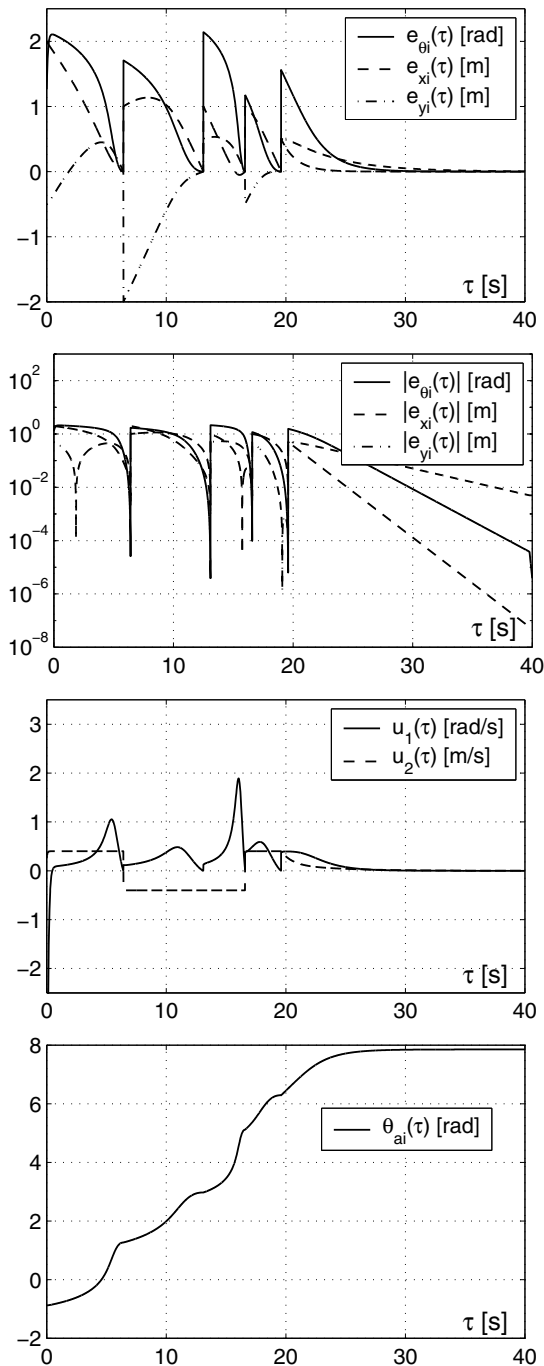


Fig. 7. SimB: time plots of signals obtained in the simulation B.

count using the scaling procedure described in (Michałek and Kozłowski, 2009).

Acknowledgment

This work was sponsored by the Polish Ministry of Science and Higher Education by the grant no. R02 009 02 (KBN-93/513).

References

- Astolfi, A. (1996). *Asymptotic Stabilization of Nonholonomic Systems with Discontinuous Control*, Ph.D. thesis, Swiss Federal Institute of Technology, Zurich.
- Bhat, S. P. and Bernstein, D. S. (2000). Finite-time stability of continuous autonomous systems, *SIAM Journal on Control and Optimization* **38**(3): 751–766.
- de Luca, A., Oriolo, G. and Samson, C. (1998). Feedback control of a nonholonomic car-like robot, in J. P. Laumond (Ed.), *Robot Motion Planning and Control*, Lecture Notes in Control and Information Sciences, Vol. 229, Springer, Berlin/Heidelberg, pp. 171–253.
- Fleury, S., Soueres, P., Laumond, J. and Chatila, R. (1995). Primitives for smoothing mobile robot trajectories, *IEEE Transactions on Robotics and Automation* **11**(3) 441–448.
- Kozłowski, K. and Pazderski, D. (2004). Modeling and control of a 4-wheel skid-steering mobile robot, *International Journal of Applied Mathematics Computer Science* **14**(4): 477–496.
- Lawrence, D. A., Frew, E. W. and Pisano, W. J. (2008). Lyapunov vector fields for autonomous UAV flight control, *AIAA Journal of Guidance, Control, and Dynamics* **31**(5): 1220–1229.
- Madi, M. (2004). Closed-form expressions for the approximation of arclength parameterization for Bezier curves, *International Journal of Applied Mathematics Computer Science* **14**(1): 33–41.
- Michałek, M. and Kozłowski, K. (2008). Motion planning and its realization using VFO stabilizer features for a differentially driven robot, in K. Tchoń and C. Zieliński (Eds.), *Problemy robotyki, Prace naukowe, Elektronika*, Vol. 166, II, Warsaw University of Technology Press, pp. 525–534, (in Polish)
- Michałek, M. and Kozłowski, K. (2009). Vector-field-orientation feedback control method for a differentially-driven vehicle, *IEEE Transactions on Control Systems Technology*, DOI: 10.1109/TCST.2008.2010406, (in print).
- Morin, P. and Samson, C. (2003). Practical stabilization of driftless systems on Lie groups: The transverse function approach, *IEEE Transactions on Automatic Control* **48**(9): 1496–1508.
- Reeds, J. A. and Shepp, L. A. (1990). Optimal paths for a car that goes both forwards and backwards, *Pacific Journal of Mathematics* **145**(2): 367–393.
- Samson, C. (1992). Path following and time-varying feedback stabilization of a wheeled mobile robot, *Proceedings of the International Conference ICARCV'92*, Singapore, pp. 13.1.1–13.1.5.
- Sasiadek, J. and Duleba, I. (1995). Local trajectory planner, *Proceedings of the AIAA Guidance, Navigation and Control Conference, Baltimore, MD, USA*, pp. 1474–1483.
- Scheuer, A. and Fraichard, T. (1997). Continuous-curvature path planning for car-like vehicles, *Proceedings of the International Conference of Intelligent Robots and Systems, Grenoble, France*, pp. 997–1003.

Siegwart, R. and Nourbakhsh, I. R. (2004). *Introduction to Autonomous Robots*, The MIT Press, Cambridge, MA.

Sordalen, O. J. and de Wit, C. C. (1993). Exponential control law for a mobile robot: extension to path following, *IEEE Transactions on Robotics and Automation* 9(6): 837–842.



Maciej Michałek received the M.Sc. and Ph.D. degrees in automatics and robotics from the Poznań University of Technology (PUT), Poland, in 2001 and 2006, respectively. He is an assistant professor at the Chair of Control and Systems Engineering of the PUT, where he lectures and conducts research. His current research interests include control theory and applications for nonlinear, nonholonomic and robotic systems.



Krzysztof Kozłowski received the M.Sc. degree in electrical engineering from the Poznań University of Technology (PUT), Poland, and the Ph.D. degree in control engineering in 1979 from the same university, where he currently holds a full professorial position in robotics and automation. In 1993, he was a Fulbright scholar with the Jet Propulsion Laboratory, Pasadena, USA. He founded and serves as a chairman of the newly established Institute of Control and

Systems Engineering at the Poznań University of Technology. He lectures and conducts research in the area of the modeling and control of industrial and mobile robots. His research interests include multi-agent systems, identification, and various robotics applications. His research publications include more than 140 conference papers and over 30 papers published in national and international journals. He is the author of the book *Modelling and Identification in Robotics* (Springer-Verlag, 1998). He was an associate editor for *IEEE Transactions on Control Systems Technology* (1999–2008), *IEEE Robotics and Automation Magazine* (1998–2002), and the *Journal of Intelligent and Robotic Systems* (2005–ongoing).

Appendix

Derivation of the left-hand side equation of (38). Recalling (37), one can write

$$\begin{aligned} \mathbf{r}_i &= \mathbf{h}_i^* - \mathbf{g}_2^* \bar{u}_2 = \begin{bmatrix} h_{2i} \\ h_{3i} \end{bmatrix} - \begin{bmatrix} \bar{u}_2 c\theta \\ \bar{u}_2 s\theta \end{bmatrix} \\ &= \|\mathbf{h}_i^*\| \begin{bmatrix} \frac{h_{2i}}{\|\mathbf{h}_i^*\|} - c\alpha_i c\theta \\ \frac{h_{3i}}{\|\mathbf{h}_i^*\|} - c\alpha_i s\theta \end{bmatrix}, \end{aligned}$$

where the notation $c\beta \equiv \cos \beta$, $s\beta \equiv \sin \beta$ is used. Next, it is easy to calculate the norm of the vector \mathbf{r}_i :

$$\begin{aligned} \|\mathbf{r}_i\|^2 &= \|\mathbf{h}_i^*\|^2 \left[\frac{h_{2i}^2}{\|\mathbf{h}_i^*\|^2} - \frac{2h_{2i}c\alpha_i c\theta}{\|\mathbf{h}_i^*\|} + c^2\alpha_i c^2\theta \right. \\ &\quad \left. + \frac{h_{3i}^2}{\|\mathbf{h}_i^*\|^2} - \frac{2h_{3i}c\alpha_i s\theta}{\|\mathbf{h}_i^*\|} + c^2\alpha_i s^2\theta \right] \\ &= \|\mathbf{h}_i^*\|^2 \left[1 - 2c\alpha_i \frac{h_{2i}c\theta + h_{3i}s\theta}{\|\mathbf{h}_i^*\|} + c^2\alpha_i \right] \\ &= \|\mathbf{h}_i^*\|^2 (1 - 2c\alpha_i c\alpha_i + c^2\alpha_i) \\ &= \|\mathbf{h}_i^*\|^2 (1 - c^2\alpha_i) \end{aligned}$$

and, finally,

$$\|\mathbf{r}_i\| = \|\mathbf{h}_i^*\| \sqrt{1 - c^2\alpha_i} = \|\mathbf{h}_i^*\| \gamma_i(\theta).$$

Calculation of the limit in (38) Knowing that $\cos \alpha_i = (\mathbf{g}_2^{*T}(\theta)\mathbf{h}_i^*)/(\|\mathbf{g}_2^*(\theta)\| \|\mathbf{h}_i^*\|)$, one can obtain

$$\begin{aligned} \gamma_i^2(\theta) &= 1 - c^2\alpha_i(\theta) \\ &= 1 - \frac{(h_{2i}c\theta + h_{3i}s\theta)^2}{\|\mathbf{h}_i^*\|^2 \|\mathbf{g}_2^*\|^2} \\ &= \frac{h_{2i}^2 + h_{3i}^2 - (h_{2i}c\theta + h_{3i}s\theta)^2}{h_{2i}^2 + h_{3i}^2} \\ &= \frac{(h_{2i}s\theta - h_{3i}c\theta)^2}{h_{2i}^2 + h_{3i}^2}. \end{aligned}$$

For $\theta(\tau) \rightarrow \theta_{ai}(\tau)$, according to (22) we have

$$\lim_{\theta \rightarrow \theta_{ai}} \tan \theta = h_{3i}/h_{2i} \Rightarrow \lim_{\theta \rightarrow \theta_{ai}} s\theta = (h_{3i}c\theta)/h_{2i},$$

which, substituted into the preceding equation, allows concluding that $\lim_{\theta \rightarrow \theta_{ai}} \gamma_i(\theta) = 0$.

Received: 16 December 2008

Revised: 18 July 2009